Journal of the Neurological Sciences 366 (2016) 37–43

Contents lists available at ScienceDirect

Journal of the Neurological Sciences

journal homepage: www.elsevier.com/locate/jns

Multi-parametric analysis assists in STN localization in Parkinson's patients

A.W. Przybyszewski [a,c,*], P. Ravin [d], J.G. Pilitsis [b], A. Szymanski [c], A. Barborica [e,f], P. Novak [g]

[a] Dept. of Neurology, University of Massachusetts, Medical School, Worcester, MA, USA
[b] Dept. of Neurosurgery, University of Massachusetts, Medical School, Worcester, MA, USA
[c] Polish–Japanese Academy of Information Technology, Warsaw, Poland
[d] Dept. of Neurology, UCLA School of Medicine, Los Angeles, USA
[e] Dept. of Research & Compliance, FHC, Inc., Bowdoin, ME, USA
[f] Dept. of Engineering, FHC, Inc., Bowdoin, ME, USA
[g] Dept. of Neurology, Brigham and Women's Faulkner Hospital, Harvard Medical School, Boston, USA

ARTICLE INFO

Article history:
Received 8 December 2015
Received in revised form 20 April 2016
Accepted 22 April 2016
Available online 23 April 2016

Keywords:
Parkinson disease subthalamic nucleus
Deep brain stimulation
Microelectrode
Multi-unit activity
Local field potentials

ABSTRACT

Background: Initial subthalamic nucleus (STN) localization is based on MRI and an anatomical atlas and then refined intraoperatively using electrophysiological mapping with microelectrode recordings (IOA – intraoperative multi-unit activity) during deep brain stimulation (DBS) in Parkinson's disease (PD). IOA is time consuming and subjective. The purpose of this study was to assess the value of high frequency multi-unit background activity (MUA, frequency >500 Hz), and local field potentials (LFP, frequency 5–500 Hz) in detection of the STN borders.
Methods: This was a retrospective, single center study. 18 leads in ten PD patients that underwent STN DBS surgery were evaluated. IOA, MUA and LFP have been compared in detection of the STN. IOA using single train spikes analysis have been used as a gold standard.
Results: Both LFP in beta range (20–35 Hz) and MUA increased as the microelectrode entered the STN and their increase correlated with dorsal/ventral STN borders. The differences (mean ± sd) were: between IOA and MUA of the dorsal/ventral border 0.20 ± 0.76/0.28 ± 0.30 mm; between IOA and LFP of the dorsal/ventral border 0.08 ± 0.94/0.05 ± 0.53 mm. Using Bland–Altman statistics, only 2 / 36 (5.6%) differences between IOA and MUA and also 2 / 36 differences between IOA and LFP (one for the dorsal border and one for the ventral border) were out of ±1.96 SD line of measurement differences. Correlation between dorsal border/ventral border positions obtained by IOA and MUA was 0.86, $p < 0.000005$/0.97, $p < 10^{-11}$; by IOA and LFP was 0.78, $p < 0.00015$/0.88, $p < 0.000001$.
Conclusions: Both MUA and LFP are characteristically elevated in the STN compared to neighboring structures. They may provide fast, real-time, objective and reliable markers of STN borders.

1. Introduction

Recordings of neuronal activity in patients with Parkinson's disease (PD) help to refine the localization of the subthalamic nucleus (STN) during deep brain stimulation (DBS) surgeries [1]. The standard microelectrode recording (MER) and intraoperative analysis of multi-unit activity (IOA) is primarily based on visual and auditory evaluations of changes in spike frequencies and background activity when a microelectrode enters STN [2,3]. Typically, MER begins about 10–20 mm above where STN is expected on the anatomical basis of the MRI. There are also changes in patterns of the spike trains when the microelectrode trajectory passes through the thalamus, zona incerta, and H2 field of Forel, STN, and the substantia nigra. Relatively sudden increases in the background activity and of neuronal spiking frequency (i.e. tonic and with occasional bursts 20–50 Hz frequency discharges) are signs that the microelectrode is in or near the STN. Kinesthetic responses and microstimulation are often used to confirm the electrode position. However, IOA is subjective and requires experience in neurophysiology, while anatomy varies by patient and often more than one microelectrode pass is needed to find the motor region of the STN. In order to avoid this problem some surgeons use 4–5 microelectrode insertions simultaneously. This may increase the chance of finding the STN and better motor effects in comparison with a single recording electrode, but clinical outcomes of 55 PD patients demonstrated that multiple recording microelectrodes induced specific mild declines in neuropsychological functions [4]. Any stimulation/manipulation of the non-motor STN is usually avoided since it can provoke psychiatric and cognitive dysfunctions. The purpose of this work was to find an alternative, less subjective means of identifying the length of STN on a given IOA semi-automatically.

* Corresponding author at: Dept. of Neurology, University of Massachusetts Medical School, 55 Lake Av North, Worcester, MA 01665, USA.

http://dx.doi.org/10.1016/j.jns.2016.04.043
0022-510X/

Quantitative analysis of microelectrode recordings using neuronal background activity has been used to facilitate the determination of STN borders [5–10]. The neuronal background has two components: high frequency multi-unit activity (MUA) defined as the despiked neuronal activity with method frequencies above 500 Hz and local field potentials (LFP). LFP are neuronal activity within the 5–500 Hz range. Previous studies indicate that both MUA and LFP can be useful in detection of the STN border [5–10].

There are no studies comparing MUA and LFP in detection of the STN borders. In this study, we hypothesized that a combination of the MUA and LFPs may improve the localization of the STN as these indices of neuronal activity may complement each other. MER has been used as a gold standard.

2. Material and methods

2.1. Study design

This is a continuation of our prospective, single-center blinded study comparing standard IOA with MUA [10] and LFP. The study was approved by the Institutional Review Board at the University of Massachusetts and all subjects signed the consent form.

2.2. Study subjects

Patients who were candidates for DBS surgery for PD at University of Massachusetts were offered participation in this study. Their candidacy was determined by a multidisciplinary group and included: PD with motor complications and/or inadequate response to medications, PD for a minimum of 5 years prior to surgery and a Hoehn and Yahr score of 2–3 [11]. Exclusion criteria were significant depression, psychosis and cognitive deficit on pre-operative neuropsychological testing. All patients underwent neuropsychological testing and Unified Parkinson Disease Rating Scale (UPDRS) in the 'on' and 'off' state to ensure dopaminergic response preoperatively. After obtaining informed consent, the patient underwent surgery.

2.3. Stereotactic surgery

Surgical planning has been previously described [10]. Briefly, patients underwent Leksell frame placement (Elekta Instruments, Atlanta GA) and CT images were merged with MRI on the BrainLab iPlan Stereotaxy 2.6 (BrainLAB AG, Feldkirchen, Germany).

All surgeries were performed with minimal local and IV sedation with dexmedetomidine, which was stopped 20 min prior to recording. They were off dopaminergic medications for at least 12 h. Localization of the STN was based on a combination of direct and indirect targeting. With stereotactic coordination in relationship to the midcommisural point, the STN was assumed to be at 11.5 mm lateral, 2.5 mm posterior and 5 mm below [12], based on our modification of standard targets. According to the Schaltenbrand and Wahren atlas [13] the usual trajectory penetrated the following structures: the anterior thalamus, the zona incerta, the H2 field of Forel, STN, and the substantia nigra (SN).

2.4. DBS electrode's contacts positions and stimulation effects

As described previously in detail [16,17], MRI, DTI and CT standard measurements were registered and tractography was performed using 3DSlicer (Harvard Medical School, Boston, MA) with the help of anatomical atlases [18,19]. Coregistration of the postoperative and preoperative images acquired via MRI or CT was performed [16] with the appropriate corrections ('BRAINFit' module of the 3DSlicer). In the next step the DTI dataset was added and a region of interest (ROI) was localized around one of the DBS electrode's contact. By using the Tractography Interactive Seeding module (3D Slicer) a tract was generated for this particular ROI [17]. We focused on regions of primary and supplementary motor cortices (regions: lip, hand, and foot) somatotopic representations [20,21]. In the next step, resultant tracts were related to the neurological observation during the initial DBS programming procedure performed by one of us (PR).

2.5. Microelectrode recording

Neural signals were recorded by using one or two simultaneous tungsten monopolar microelectrodes (22675Z, FHC, Inc., Bowdoin, ME) with impedance in the range of 0.4 to 0.9 MΩ. The electrodes were advanced by the Microdrive (microTargeting Drive, FHC, Inc., Bowdoin, ME) and signals were recorded using the Guideline 4000 (FHC, Inc., Bowdoin, ME). Recordings were started 20 mm above the target with a microelectrode that was advanced in 0.5 mm increments to between 20 and 10 mm above the target and later increments were 0.3 mm. Ten second recordings were obtained at each point. The Guideline 4000 recording system allows recording of MUA and LFP simultaneously and from the same microelectrode tip. Recordings were digitized at 24 kHz for MUA, and then downsampling was performed by averaging 24 samples of the wideband signal, to obtain a second LFP stream having a 1000 Hz sampling rate from a primary stream recorded at 24 kHz. This method ensures that HFBA and LFP are recorded at the EXACT SAME LOCATION, the microelectrode tip. That allows us to directly compare the localization accuracy of the two measures. Recorded signals were band-pass filtered at high frequencies (300 Hz to 5 kHz) for recordings of spikes with background activity and at low frequencies (5–500 Hz) for LFP signals, and stored for offline analysis. All filtering has been performed in real-time by the digital signal processors of the recording system, using zero-phase digital filters, such that the HFBA and LFP streams were not only recorded at the same location, but they were also in perfect phase alignment.

Increases in the background neural activity and in the neuronal firing, and/or alteration of neural firing by passive movement of contralateral limbs were used to distinguish the STN and its borders. Another track was undertaken if the STN length was <3 mm, if background neuronal activity was lower than expected, and/or if kinesthetic responses were absent. In the next step, microstimulation was performed to evaluate potential side effects. Once the optimal trajectory and target were chosen, a lead was implanted (Model 3389, Medtronic Inc, Minneapolis, MN) and macrostimulation was performed up to 9 V to confirm contralateral improvement of rigidity, tremor, or bradykinesia. Lead position was documented with postoperative MRI.

2.6. Data processing

Off-line signal processing software was written in Matlab (Matworks, Natick, MA). The parts of recordings with artifacts were removed when the calculated RMS (root mean square) of the signal significantly increased (MUA was analyzed by modification of the method described in details earlier [9]). In short, large spikes were extracted and removed with the wavelet method (unsupervised Daubechies-based wavelet denoising algorithm with soft-thresholding as described before [10,14]) without changing the background activity.

The power spectral density for MUA was calculated over 10-second segments of despiked neuronal activity using Welch's method [22] with a Fourier transform window length of 6000 samples per segment, weighted by means of a Hamming window. As before, the HFBA was obtained by integrating the 500–2000 Hz band in the power spectral density [10].

The lengths of segments were determined to achieve minimal noise and fluctuations of the dominant frequencies between segments (as the time-frequency analysis – ridges – have demonstrated that LFP [23] as well as EEG [24] signals have variable periods of the dominant frequencies). The power spectral density for LFP was calculated from segments of at least about 1 s duration with a Fourier transform of the signal weighted by a Hanning window. Low frequency signals (related to the

LFP) were divided into 512 up to 4096 points segments with 50% overlap, weighted by a Hanning window and averaged. The 10-second recordings of LFPs were normally divided into 4096-sample segments with 50% overlap, weighted by a Hanning window and averaged. Whenever shorter segments (>1 s) had to be selected, we have decreased the window length down to 512 samples, in order to use Welch's method [22] over a minimum of three windows per analyzed segment. The length of the segments was 1.024 s. We have applied Welch's method [22] in an attempt to reduce the noise in the power estimate. The shorter the window, the lower the frequency resolution, roughly, for the window's length 512 @ 1 kH sampling, the frequency resolution is above 2 Hz. However, that should affect the fine details at the edges of the band over which we integrate the power, at the expense of reduced noise.

We have used different windows of analysis (constant for each subject) because we were limited in our LFP analysis to relatively short 10 s periods and results of the FFT transformations of the whole 10 s segments were not very stable (fluctuations). The LFP was obtained by integrating 20–35 Hz bands in the power spectral density.

The criteria for the STN borders were similar for both methods. The dorsal border was defined as the first site along a track where the integrated power spectra amplitude for high (MUA) or for low (LFP) frequencies exceeded the baseline amplitude by at least 50% and elevation/oscillations of the amplitude were sustained for MUA/LFP. The baseline amplitude was obtained as an average amplitude from recordings of 10 mm above the target that usually corresponds to the thalamic activity. The ventral border was defined as the last site along a track where the amplitude reduction or oscillations were <50% compared to the average amplitude within the STN.

After completing each surgery, the deidentified MER's were analyzed off-line and the LFP and MUA analysis was blinded to the IOA.

2.7. Statistical analysis

The dorsal and ventral borders obtained by each technique were compared using Pearson's correlation analysis, ANOVA analysis of variance and Bland–Altman statistics [15] to compare the two diagnostic methods. Bland–Altman plots allow us to investigate the existence of any systematic difference between the measurements (i.e., fixed bias) and to identify possible outliers. The mean difference is the estimated bias, and the SD of the differences measures the random fluctuations around this mean. If the mean value of the difference differs significantly from 0 on the basis of a 1-sample *t*-test, this indicates the presence of fixed bias. In order to estimate how far apart the measurements were using different methods, we have computed 95% limits of agreement for each comparison (average difference ± 1.96 standard deviation of the difference).

Matlab (Matworks, Natick, MA) statistical toolbox was used for all statistical analyses.

3. Results

3.1. Demographics

Our cohort consisted of 7 men and 3 women. The mean and standard deviation (SD) age was 56 ± 11 years and duration of disease 11 ± 5 years. The mean motor score UPDRS III off and on medication was 59 ± 8 and 29 ± 10 respectively. Levodopa equivalent (mean ± sd) was 934.7 ± 410.1 before the surgery and 716.1 ± 257.0 after the surgery. Nine patients had bilateral STN implantation; one only unilateral. In one patient with bilateral implantation, LFP from only one side were available. In two patients, we used two microelectrodes simultaneously on both sides and one on each side in all other patients; we used single microelectrode recordings. All patients tolerated the procedure well. Intraoperative macrostimulation confirmed good placement. Lead position was verified with MRI [10] (Fig. 1). The neurologist determined the active contact with the best response in DBS programming and typically the active contact was 1 or 2.

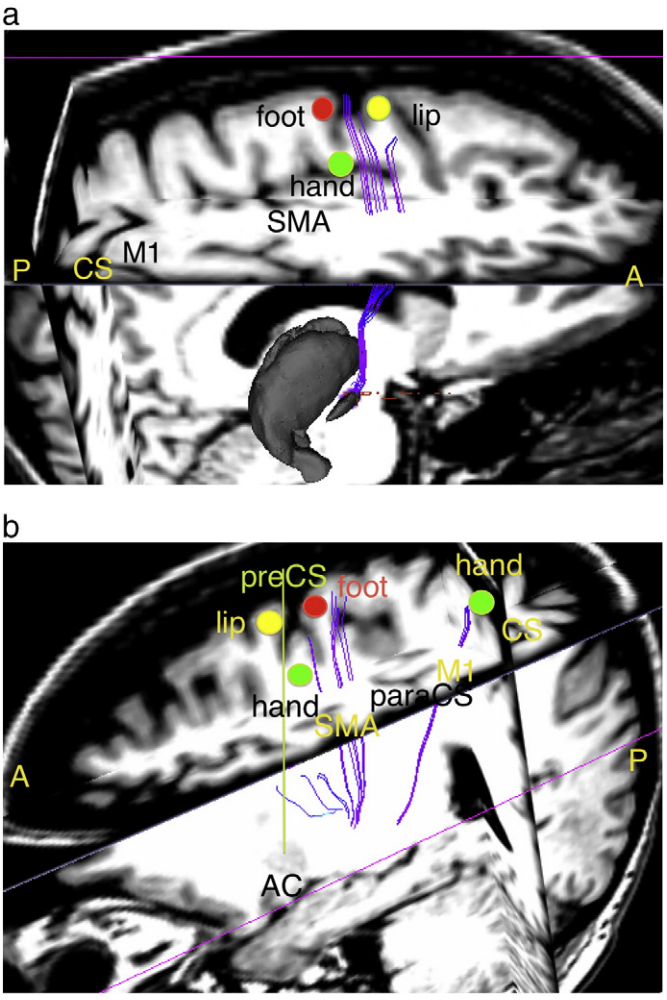

Fig. 1. Sagittal MRI with overlay partial axial and coronal parts for Pat #7 a) left; b) right side. In a) also anatomical images of the thalamus and STN from SPL and 3D atlas [17,18] were overlaid. Tractography was generated from contact 1 on the basis of MRI/DTI images as described in details [16]. CS - central sulcus, para-CS – paracentral sulcus; pre-CS – precentral sulcus, AC – anterior commiserate, A – anterior, P-posterior, M1-primary motor cortex, SMA – supplementary motor cortex; hand, foot and lip – approximate position of M1 or SMA somatotopic projections.

The mean number of tracks were 1.3 ± 0.5 on the left and 1.2 ± 0.4 on the right. A total of 51 tracks were recorded. Optimal STN was detected in 36 tracks. Fifteen tracks were considered suboptimal based on the IOA using MUA, but not LFP (Figs. 2 and 3). In a typical optimal track, the MUA abruptly increased compared to the thalamic/zona incerta activity as the electrode penetrated the dorsal border of the STN. The MUA level varied within the STN but typically remained above the thalamic/zona incerta level. LFP however did not always show a higher mean value in the STN but in most cases did have high amplitude oscillations in STN (Figs. 2, 3). Both MUA and LFP significantly decreased outside the borders of the STN. Examples of simultaneously recorded MUA and LFP in comparison to IOA are shown in Figs. 2–3. Both figures demonstrate recordings from two simultaneous microelectrodes involving different patients. In the patient in Fig. 2, the center track demonstrated more STN than the lateral track by IOA as determined by both the OR and outside teams. LFP are similar for both microelectrodes and LFP power oscillations are also similar. In the patient in Fig. 3, LFP of both the anterior and center track suggest STN while typical MUA is present only in the anterior. LFP peak occurs earlier in the center track as compared to anterior. IOA are shown in Figs. 2–3. Both figures are showing

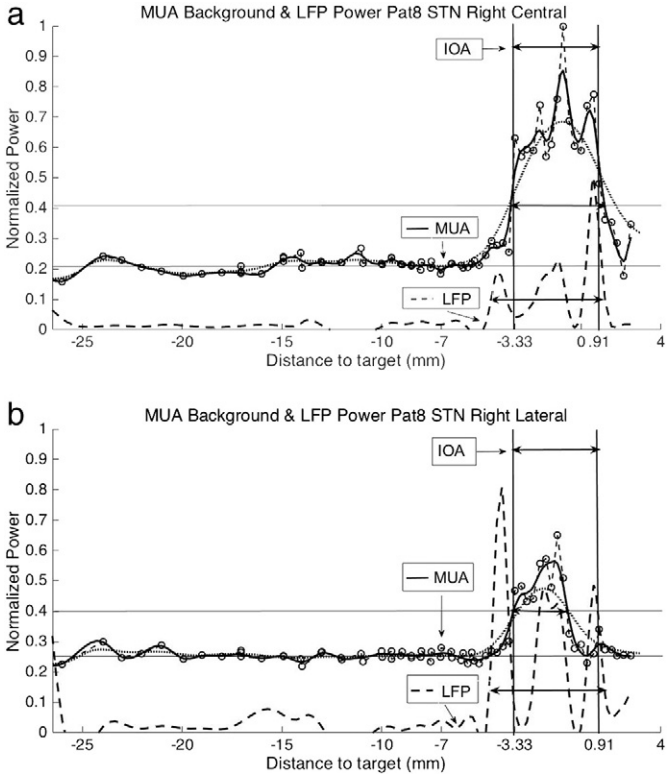

Fig. 2. An example of IOA, MUA and LFP recordings by two microelectrodes; a) central, and b) lateral electrodes (Pat #8R). IOA is similar to MUA, but LFP increased more dorsal than IOA in a). In b) IOA was taken from the central electrode, but STN is thinner (MUA), however LFP is same as in a).

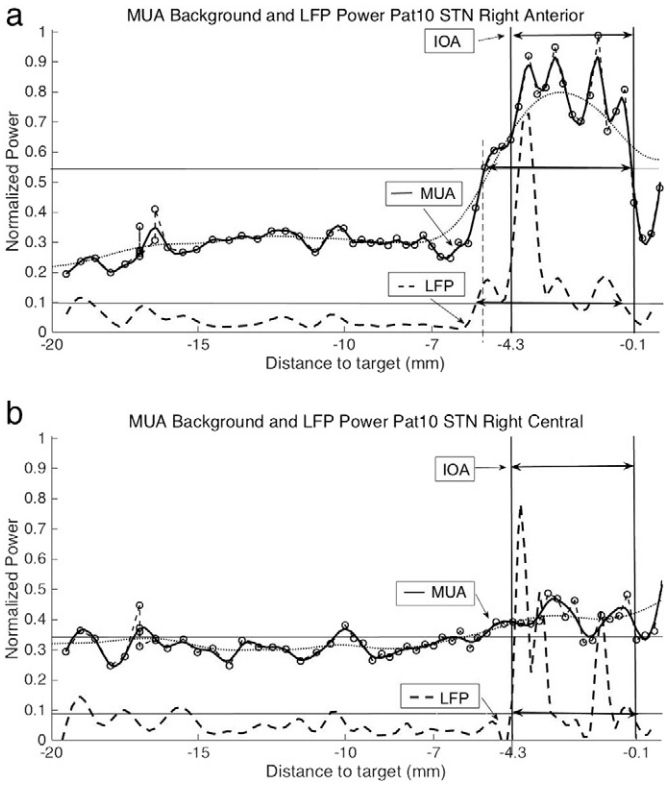

Fig. 3. An example of IOA, MUA and LFP recordings by two microelectrodes; a) anterior, and b) central electrodes (Pat #10R). Similar to Fig. 2 LFP is more dorsal than IOP, but v interesting is in b): IOA is from a) and there is no increase of MUA that means that microelectrode is outside STN, but LFP is showing changes in the amplitude similar to (a) suggesting that the electrode is inside STN.

recordings from two microelectrodes in two different patients. In patient #8, right side, the central microelectrode went through the central part of the STN, whereas the lateral electrode passed a smaller STN part. IOA is the same for both electrodes as it was obtained intra-op by the neurosurgeon for the central microelectrode. It is interesting that LFP are similar for both microelectrodes and LFP power oscillations are also similar. Even more interesting is the case of patient #10 right (Fig. 3) where LFP show STN in both anterior and central microelectrodes but MUA only in the anterior one. However, in the central microelectrodes LFP signal is shifted dorsally in comparison to the anterior electrode LFP signal.

We next examined the measurements of the STN dorsal and ventral borders obtained by all three methods separately for each side and subject (Fig. 4) or as means (Fig. 5). The mean differences between IOA and MUA of the dorsal/ventral border were $0.20 \pm 0.76/0.28 \pm 0.30$ mm; between IOA and LFP of the dorsal/ventral border $0.08 \pm 0.94/0.05 \pm 0.53$ mm; between MUA and LFP of the dorsal/ventral border.

$0.28 \pm 0.80/0.33 \pm 0.50$ mm. One-way ANOVA determined that there is no difference in measure characteristic between left (L), right (R) dorsal (L: $F = 0.16$, $p = 0.86$; R: $F = 0.3$; $p = 0.74$) and left (L), right (R) ventral (L: $F = 0.19$, $p = 0.83$; R: $F = 0.07$, $p = 0.93$) MER, MUA and LFP values.

On the basis of mean values it seems that LFP better approximates IOA than MUA. In order to verify this we have calculated mean absolute differences between IOA and MUA of the dorsal/ventral border which were $0.47 \pm 0.38/0.30 \pm 0.28$ mm; between IOA and LFP of the dorsal/ventral border $0.70 \pm 0.61/0.43 \pm 0.30$ mm; between MUA and LFP of the dorsal/ventral border $0.61 \pm 0.57/0.45 \pm 0.36$ mm. (Fig. 4).

For the Bland–Altman statistic, we considered the threshold 1.96 of standard deviations of differences between both methods as 95% limits

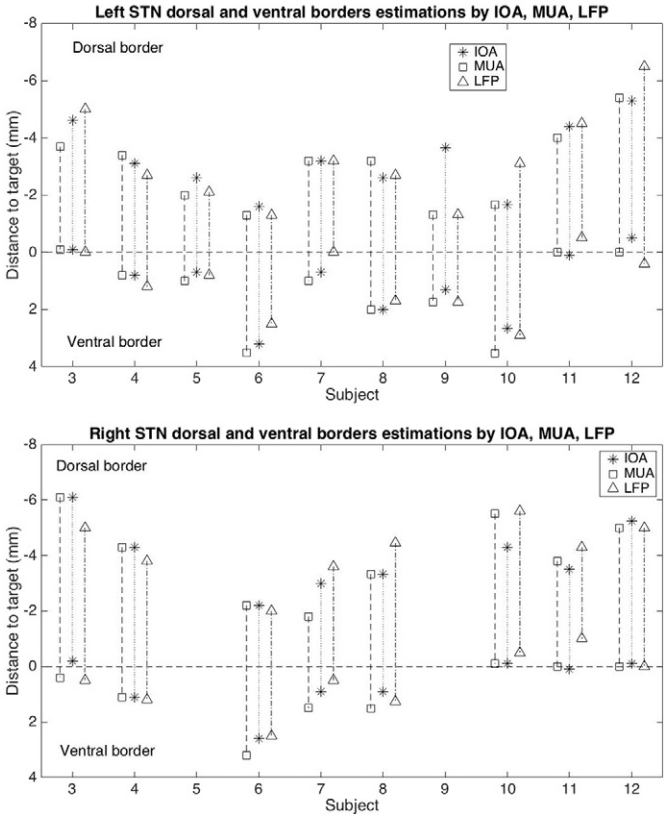

Fig. 4. Comparison of the STN boarder detection by IOA, MUA, and LFP. Each point represents localization of the STN ventral and dorsal boarders in one subject. The values above the anatomical target at 0 mm are positive; values below the target are negative. Only the best track is shown when simultaneous recordings of more than one track were performed.

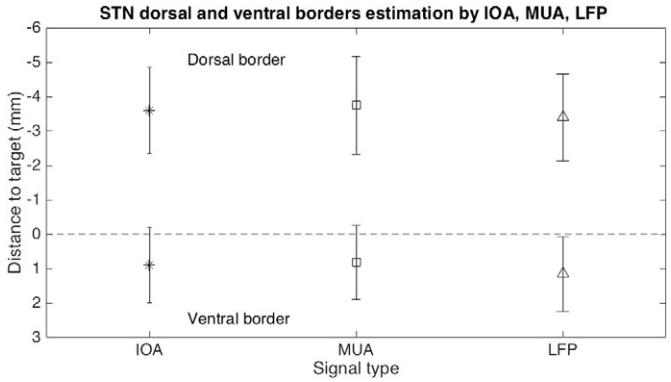

Fig. 5. Comparison of the STN boarder detection by IOA, MUA, and LFP. Each point represents localization of the STN ventral and dorsal borders as a mean ± SD for all subjects. The values above (dorsal to) the target as defined by imaging at 0 mm are negative; values below (ventral to) the target are positive.

of agreement for each comparison. We have performed separate analysis for dorsal and ventral STN (Fig. 6). For both STN borders LFP has larger SD differences compared to MUA differences from IOA, but the mean difference is smaller for LFP than MUA (Fig. 6). There were only 2 / 36 (5.6%) data points that met criteria for <1.96 SD. Differences (one for the dorsal border and one for the ventral border) exceeded ±1.96 SD line of measurement differences for MUA and also for LFP. These results can be interpreted to suggest that MUA and IOA as well as LFP and IOA methods are in reasonable agreement [15].

Correlation between dorsal/ventral border positions obtained by IOA and MUA was 0.86, $p < 0.000005/0.97$, $p < 10^{-11}$; by IOA and LFP was 0.78, $p < 0.00015/0.88$, $p < 0.000001$. We have also calculated correlation between dorsal/ventral border positions obtained by LFP and MUA as 0.86, $p < 0.000006/0.92$, $p < 6*10^{-8}$.

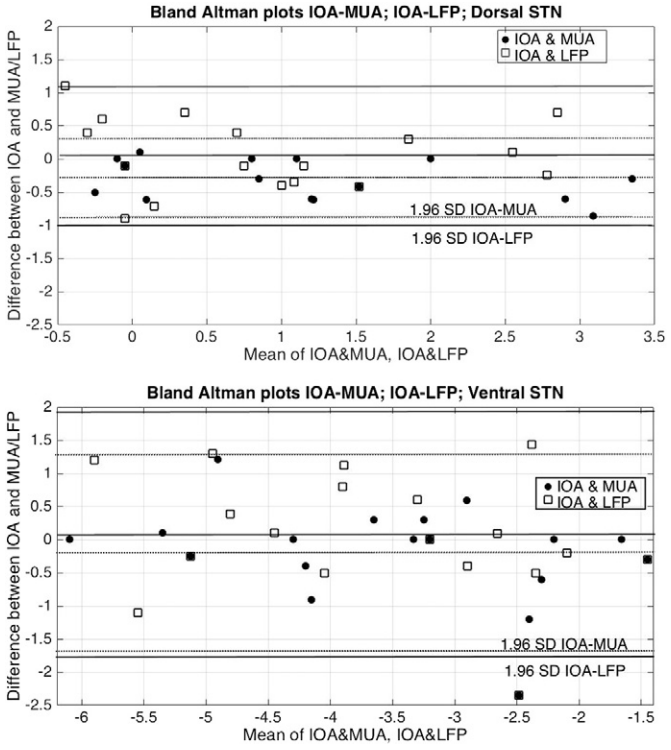

Fig. 6. Bland Altman plots comparing STN border estimation by IOA and MUA, and IOA and LFP for dorsal (upper plot) and ventral (lower plot) STN borders.

3.2. MRI/DTI and neurological symptoms

In the previous study [10] the placement of the DBS leads was verified by the postoperative MR imaging in order to confirm that contacts of the DBS electrode were in the STN (see Fig. 1 in [10]). In this report we have performed a more advanced conformation of the electrode placement and tried to verify not only that contacts are near/in STN but which part of the STN is stimulated by a particular contact. We were also able to find which pathways might be stimulated by each contact. Moreover, on the basis of the literature and somatotopic projections in M1 and SMA we were able to determine to which specific motor areas the pathways are going.

In one example we have demonstrated the effectiveness of the stimulation for patient #7 (Fig. 1). Patient #7 had been diagnosed with PD 9 years ago.

Before surgery (*Pre-OP*): Pat #7 symptoms started on the left side with dystonic cramps in both feet, freezing gait, falls, mild depression, hypometric saccadic pursuit, and limited head rotation to R plus rigidity. *Post-OP*: *Left side stimulator*: case + contact #1-, 2.5 V: improved dexterity and normalized limb tone in the right upper extremity (RUE), restless leg symptoms when 'off'. Compare post-op symptoms with trajectories from STN contact 1 to hand area in M1 and SMA, as well as to foot area in SMA (Fig. 1). *Right side stimulator*: case + contact #1-, 2.5 V: good rhythmicity on repetitive tapping LUE (left upper extremity) – decreased tone in the left shoulder/no weakness. Notice projections are from STN contact #1 to foot and hand areas in SMA (Fig. 1).

4. Discussion

This study directly compared the ability of MUA and LFP to localize STN using IOA as a reference. All three methods had reasonable agreement of STN borders and strongly correlated. These results indicate that the assessment of the STN borders using MUA/LFP is not only objective but also accurate. The main strength of our study is its' prospective nature. Hence the experimental bias associated with our previous retrospective study [9] was eliminated. It should be stressed that there were no false positive detections of the STN by MUA and there was 100% agreement in missed tracks using both methods.

LFP signal (Fig. 3) may increase as the dorsal STN border is approached. Additionally, it may be able to confirm even in less optimal tracks that STN is within 2 mm. In both Figs. 2 and 3, LFP increased in short and missed segments. This finding is helpful to the surgeon as a means of assurance that the STN is near the microelectrode pass. Moving forward, signatures of LFP from missed tracks may be obtained and potentially aid the surgical team to determine in which direction the next track should be made.

One limitation of this study is that all comparisons were performed off-line. Of note, however, these results can be available within hundreds of milliseconds and the algorithm can be easily implemented in real time. Our study also suggests that 10 s of IOA for BA such as MUA and LFP is adequate for the STN localization. This is a much shorter period than needed by most experts; as in our usual protocol, where we typically obtain 65 recording sites per track. Thus algorithmic STN detection may significantly shorten DBS surgeries. The operating room time could be further reduced if the need to test kinesthetic cells could be decreased by determining MUA/LFP signatures. The idea of automatic IOA being used to streamline recordings, limit bias, and standardize the procedures (and hopefully the outcomes) is exciting and could aid less experienced teams in performing DBS. An interesting perspective would be to completely automatize microelectrode recordings by using feedback between analysis of recorded signals and the next microelectrode advancement step. The microelectrode could move with larger steps at the beginning and change step size automatically when signals show that it is near STN. Such an approach would make STN surgeries faster and easier for less experienced neurosurgical teams.

While there are few papers exploring utility of the MUA changes [6,10,25–27] there are more papers related to the LFP changes correlating with STN borders. Weinberger et al. [28] have shown that almost all (89%) of the measurements that display oscillatory spiking activities are coherent with simultaneously measured LFP. They noted dominant oscillatory activity with beta frequency (13–35 Hz) based in LFP [28–33] and elevated beta activity may be associated with bradykinesia and rigidity in PD [29]. However, it is important to note that LFP is related to slow oscillations that have lower spatial resolution than IOA signal. The LFP signal can be influenced by sources up to a distance of 10 mm depending on their frequency, the architecture of neural assemblies and their synchronization [34]. We have observed these spatial differences in our recordings, especially in Fig. 3b where a microelectrode was outside STN – there was no MUA signal, but we found significant LFP signal indicating that the electrode was not far from the STN.

Another important issue is placement of the electrode to stimulate the right part of the STN as stimulation of the limbic STN part may cause very strong side effects [35]. In a recent paper, Verhagen et al. [36] proposed combining recordings of LFP and neuronal spiking and calculating beta power over the coherent parts of the LFP spectrum (sensorimotor power index (SMPI) of beta frequencies) in order to find the sensorimotor STN. The method proposed by Verhagen et al. [36] is based on earlier recordings from STN [26,29].

As beta oscillation power changes with disease progression, medication and movements, Priori [37] proposed to use it in order to optimize parameters of the DBS stimulation in the post-operative condition (adaptive DBS: aDBS). Medtronic proposed a research project with the purpose of using feedback loops: parameters of DBS stimulation <-> LFP power as a permanent optimization of the DBS method (as a bi-directional brain-machine interface) [38,39]. The name of the project is Activa PC + S and the whole device would be placed in the standard stimulation box chronically implanted under skin [40].

However, in addition to the feedback-loop stimulation, we propose modification of the DBS stimulation parameters for different contacts on the basis of our Fig. 1. By finding which contact and what parameters are optimal for stimulation of different parts of the primary motor cortex and SMA (see [16,17] for details) and by comparing this with symptoms (neurological examination), we might be in a position to adapt parameters of stimulation to the individual patient and his/her individual treatment (medications) and movements (e.g. adaptive, individual gait optimization, etc.).

Our equipment allowed to record MUA and LFP simultaneously and from the same electrode. All signals were at first digitized, and then divided into the high (spikes and background activity) and LFP (details in the Material and methods section) frequency bands. This method ensures that MUA (high frequency) and LFP are simultaneously recorded at the EXACT SAME LOCATION, the microelectrode tip. That allows us to directly compare the localization accuracy of these two measures.

This was not possible for the setup in [2], using the ring for recording of LFPs that was separated from the electrode's tip (for recording of spikes).

But our method has a limitation in estimations of only STN dorsal and ventral borders positions.

As a golden standard neurosurgeons are using IOA (intraoperative multi-unit activity) as partly subjective indicator of the STN borders. Generally, IOA depends on spike activities, background noise, responses to movements, etc. Experienced team (neurosurgeon and neurologist/neuroscientist) can recognize STN borders by hearing IOA but the importance of different parameters is subjective. A neurosurgeon needs STN borders information to find by which part of the STN is the electrode passing (is the electrode in the middle or near the STN corners) and to put stimulation electrode near the ventral boarder of the STN. Notice that our signals: 1) MUA is the high frequency multi-unit background activity, so it is one of the neurosurgeon indications for STN borders under assumption that she/he is not paying attention to large spikes at this moment; 2) LFP signal is related to synaptic activities from a larger area. We have demonstrated that all signals have significant correlations in the dorsal and ventral STN borders, which is important and sufficient information for the neurosurgeon.

However, we are not able to correlate IOA with MUA or LFP signal inside the STN because we do not have values of the IOA inside the STN, only near the borders. One may find changes for example in spike activity in the STN, but one needs to separate different spike shapes into clusters and correlate them with other signals. In fact one of us has participated in such study with multi-electrode recording system and automatic classifications which microelectrode is in/out-side of the STN on the basis of clustering spike trains with the low- and high-frequency background activity [41].

5. Conclusions

Simultaneous recordings of the background activity including high frequency MUA and low frequency LFP in addition to standard IOA may improve the precision and speed of the STN border determination. Better anatomical localization may translate into improved effectiveness of the DBS by adjusting stimulation parameters to an individual patient's symptoms.

Acknowledgment

AWP was partly supported by NCN grant DEC-2011/03/B/ST6/03816.

References

[1] A.L. Benabid, S. Chabardes, J. Mitrofanis, P. Pollak, Deep brain stimulation of the subthalamic nucleus for the treatment of Parkinson's disease, Lancet Neurol. 8 (2009) 67–81.
[2] S. Marceglia, S. Mrakic-Sposta, G. Tommasi, L. Bartolomei, C. Foresti, F. Valzania, et al., Multicenter study report: electrophysiological monitoring procedures for subthalamic deep brain stimulation surgery in Parkinson's disease, Neurol. Sci. 31 (2010) 370–387.
[3] A. Benazzouz, S. Breit, A. Koudsie, P. Pollak, P. Krack, A.L. Benadib, Intraoperative microrecordings of the subthalamic nucleus in Parkinson's disease, Mov. Disord. 17 (2002) S145–S149.
[4] Y. Temel, P. Wilbrink, A. Duits, P. Boon, S. Tromp, L. Ackermans, V. van Kranen-Masternbroek, W. Weber, V. Visser-Vandewalle, Single electrode and multiple electrode guided electrical stimulation of the subthalamic nucleus in advanced Parkinson's disease, Neurosurgery 61 (2007) 346–357.
[5] A. Pesenti, M. Rohr, M. Egidi, P. Rampini, F. Tamma, M. Locatelli, et al., The subthalamic nucleus in Parkinson's disease: power spectral density analysis of neural intraoperative signals, Neurol. Sci. 24 (2004) 367–374.
[6] A. Snellings, O. Sagher, D.J. Anderson, J.W. Aldridge, Identification of the subthalamic nucleus in deep brain stimulation surgery with a novel wavelet-derived measure of neural background activity, J. Neurosurg. 111 (2009) 767–774.
[7] T. Kano, Y. Katayama, K. Kobayashi, M. Kasai, H. Oshima, C. Fukaya, et al., Detection of boundaries of subthalamic nucleus by multiple-cell spike density analysis in deep brain stimulation for Parkinson's disease, Acta Neurochir. Suppl. 99 (2006) 33–35.
[8] A. Moran, I.B. Gad, H. Bergman, Z. Israel, Real-time refinement of subthalamic nucleus targeting using Bayesian decision-making on the root mean square measure, Mov. Disord. 21 (2006) 1425–1431.
[9] P. Novak, S. Daniluk, S.A. Ellias, J.M. Nazzaro, Detection of the subthalamic nucleus in microelectrographic recordings in Parkinson disease using the high-frequency (N500 Hz) neuronal background. Technical note, J. Neurosurg. 106 (2007) 175–179.
[10] P. Novak, A.W. Przybyszewski, L. Margoli, A. Barborica, P. Ravin, J.G. Pilitsis, Localization of the subthalamic nucleus in Parkinson disease using multi unit activity, J. Neurol. Sci. 310 (2011) 44–49.
[11] A.J. Hughes, S.E. Daniel, L. Kilford, A.J. Lees, Accuracy of clinical diagnosis of idiopathic Parkinson's disease: a clinico-pathological study of 100 cases, J. Neurol. Neurosurg. Psychiatry 55 (1992) 181–184.
[12] P.A. Starr, C.W. Christine, P.V. Theodosopoulos, N. Lindsey, D. Byrd, A. Mosley, et al., Implantation of deep brain stimulators into the subthalamic nucleus: technical approach and magnetic resonance imaging-verified lead locations, J. Neurosurg. 97 (2002) 370–387.
[13] G. Schaltenbrand, W. Wahren, Atlas for Stereotaxy of the Human Brain, Georg Thieme, Stuttgart, 1977.
[14] D.L. Donoho, De-noising by soft-thresholding, IEEE Trans. Inf. Theory 41 (1995) 613–627.
[15] J.M. Bland, D.G. Altman, Statistical methods for assessing agreement between two methods of clinical measurement, Lancet 1 (1986) 307–310.
[16] A. Szymanski, A.W. Przybyszewski, The 2014 International Conference on Brain Informatics and Health (2014 BIH 8609) in: D. Slezak, L. Schwabe, A.-H. Tan, J.F.

Peter (Eds.), Rough Set Rules Help to Optimize Parameters of Deep Brain Stimulation in Parkinson's Patients, LNAI 8609 2014, pp. 345–356.
[17] A. Szymanski, A. Kubis, A.W. Przybyszewski, data mining and neural network simulation can help to improve deep brain stimulation effects in Parkinson's disease, Comput. Sci. 16 (2) (2015) 199–215.
[18] I.-F. Talos, M. Jakab, R. Kikinis, M.E. Shenton, SPL-PNL Brain Atlas, SPL, 2008.
[19] A. Krauth, R. Blanc, A. Poveda, D. Jeanmonod, A. Morel, G. Székely, A mean three dimensional atlas of the human thalamus: generation from multiple histological data, NeuroImage 49 (2010) 2053–2062.
[20] F. Cauda, G. Giuliano, D. Federico, D. Sergio, S. Katiuscia, Discovering the somatotopic organization of the motor areas of the medial wall using low-frequency BOLD fluctuations, Hum. Brain Mapp. 32 (10) (2011) 1566–1579.
[21] A.R. Mayer, J.L. Zimbelman, Y. Watanabe, S.M. Rao, Somatotopic organization of the medial wall of the cerebral hemispheres: a 3 tesla fMRI study, Neuroreport 12 (17) (2001) 3811–3814.
[22] P.D. Welch, The use of fast Fourier transform for the estimation of power spectra: a method based on time averaging over short, modified periodograms, IEEE Trans. Audio Electroacoust. AU-15 (2) (1967) 70–73.
[23] A.W. Przybyszewski, T.M. Rutkowski, Processing of the incomplete representation of the visual world, in: O. Hryniewicz, J. Kacpryzk, J. Koronacki, S. Wierzchon (Eds.), Issues in Intelligent Systems Paradigms, Akademicka Oficyna Wydawnicza EXIT, Warsaw, Poland 2005, pp. 225–235.
[24] T.M. Rutkowski, D.P. Mandic, A. Cichocki, A.W. Przybyszewski, EMD approach to multichannel EEG data—the amplitude and phase components clustering analysis, J. Circ. Syst. Comput. 19 (2010) 215–229.
[25] A.W. Przybyszewski, Deep brain stimulation, J. Neurosurg. (August 9 2013), http://dx.doi.org/10.3171/2011.2.JNS101964.
[26] Y. Miyagi, T. Okamoto, T. Morioka, S. Tobimatsu, Y. Nakanishi, et al., Spectral analysis of field potential recordings by deep brain stimulation electrode for localization of subthalamic nucleus in patients with Parkinson's disease, Stereotact. Funct. Neurosurg. 87 (4) (2009) 211–218.
[27] S.F. Danish, G.H. Baltuch, J.L. Jaggi, S. Wong, Determination of subthalamic nucleus location by quantitative analysis of despiked background neural activity from microelectrode recordings obtained during deep brain stimulation surgery, J. Clin. Neurophysiol. 25 (2008) 98–103.
[28] M. Weinberger, N. Mahant, W.D. Hutchison, A.M. Lozano, E. Moro, M. Hodaie, et al., Beta oscillatory activity in the subthalamic nucleus and its relation to dopaminergic response in Parkinson's disease, J. Neurophysiol. 96 (2006) 3248–3256.
[29] A.A. Kühn, T. Trottenberg, A. Kivi, A. Kupsch, G.H. Schneider, P. Brown, The relationship between local field potential and neuronal discharge in the subthalamic nucleus of patients with Parkinson's disease, Exp. Neurol. 194 (2005) 212–220.
[30] C.C. Chen, A. Pogosyan, L.U. Zrinzo, S. Tisch, P. Limousin, et al., Intra-operative recordings of local field potentials can help localize the subthalamic nucleus in Parkinson's disease surgery, Exp. Neurol. 198 (2006) 214–221.
[31] T. Trottenberg, A. Kupsch, G.H. Schneider, P. Brown, A.A. Kühn, Frequency-dependent distribution of local field potential activity within the subthalamic nucleus in Parkinson's disease, Exp. Neurol. 205 (2007) 287–291.
[32] I. Telkes, N.F. Ince, I. Onaran, A. Abosch, Localization of subthalamic nucleus borders using macroelectrode local field potential recordings, Conf Proc IEEE Eng Med Biol Soc. 2014 (2014) 2621–2624.
[33] I. Telkes, N.F. Ince, I. Onaran, A. Abosch, Spatio-spectral characterization of local field potentials in the subthalamic nucleus via multitrack microelectrode recordings, Conf. Proc. IEEE Eng. Med. Biol. Soc. 2015 (2015) 5561–5564.
[34] G. Buzsaki, C.A. Anastassiou, C. Koch, The origin of extracellular fields and currents—EEG, ECoG, LFP and spikes, Nat. Rev. Neurosci. 13 (2012) 407–420.
[35] L. Mallet, M. Schüpbach, K. N'Diaye, P. Remy, E. Bardinet, V. Czernecki, M.-L. Welter, A. Pelissolo, M. Ruberg, Y. Agid, J. Yelnik, Stimulation of subterritories of the subthalamic nucleus reveals its role in the integration of the emotional and motor aspects of behavior, Proc. Natl. Acad. Sci. 104 (2007) 10661–10666.
[36] R. Verhagen, D.G. Zwartjes, T. Heida, E.C. Wiegers, M.F. Contarino, et al., Advanced target identification in STN-DBS with beta power of combined local field potentials and spiking activity, J. Neurosci. Methods 253 (2015) 116–125.
[37] A. Priori, G. Foffani, L. Rossi, S. Marceglia, Adaptive deep brain stimulation (aDBS) controlled by local field potential oscillations, Clin. Exp. Neurol. 245 (2013) 77–86.
[38] S. Little, P. Brown, What brain signals are suitable for feedback control of deep brain stimulation in Parkinson's disease? Ann. N. Y. Acad. Sci. 1265 (2012) 9–24.
[39] E.J. Quinn, Z. Blumenfeld, A. Velisar, M.M. Koop, L.A. Shreve, M.H. Trager, B.C. Hill, C. Kilbane, J.M. Henderson, H. Brontë-Stewart, Beta oscillations in freely moving Parkinson's subjects are attenuated during deep brain stimulation, Mov. Disord. 30 (2015) 1750–1758.
[40] W.J. Neumann, F. Staub, A. Horn, J. Schanda, J. Mueller, G.H. Schneider, P. Brown, Kühn AA, Deep brain recordings using an implanted pulse generator in Parkinson's disease, Neuromodulation 19 (2016) 20–24.
[41] K. Ciecierski, Z.B. Ras, A.W. Przybyszewski, Foundations of automatic system for intrasurgical localization of subthalamic nucleus in Parkinson patients, Web Intell. Agent Syst. 12 (1) (2014) 63–82.